LARGE AREA *N*-TYPE CZ DOUBLE SIDE CONTACT BACK JUNCTION SOLAR CELL WITH 21.3% CONVERSION EFFICIENCY

V. Mertens, T. Ballmann, J. Cieslak, M. Kauert, A. Mohr, F. Stenzel, M. Junghänel, K. Suva, Ch. Klenke, G. Zimmermann, J. W. Müller
Hanwha Q Cells GmbH
Germany, Sonnenallee 17-21, D-06766 Bitterfeld-Wolfen

ABSTRACT: We present our work on boron emitter back junction silicon solar cells with both sided contacts and phosphorus diffused front surface field processed on 6" full square *n*-type Cz silicon. We give an analysis of the V_{oc} limitations of our solar cell structure and show that the metallized surfaces are the main contributors, followed by the passivated surfaces. To demonstrate the influence of recombination losses we show the gain in V_{oc} and J_{sc} obtained by reduction of the front metallization fraction. By implementation of similar optimization strategies we could improve our solar cells featuring rear side aluminum PVD metallization up to an efficiency of 21.3% (independently confirmed by Fraunhofer ISE CalLab). We also processed back junction solar cells with cost effective all screen printed metallization with 20.7% efficiency. Both solar cell types, PVD rear metal and all screen printed solar cells exhibit open circuit voltages larger than 670 mV. To give insight into the operation of our solar cell in the field we model the operation conditions under 1 sun and 0.1 suns and give experimental data of the low light performance and the temperature coefficients for our solar cell structure.
Keywords: *n*-type, solar cell, back junction, high level injection conditions

1 INTRODUCTION

In order to improve efficiencies of double side contacted solar cells on Czochralski (Cz) silicon based material, recently the interest in respective solar cell concepts which use *n*-type Cz silicon has increased. *N*-type Cz silicon exhibits high minority carrier lifetimes and is more tolerant towards various metal impurities than *p*-type Cz [1]. Due to the high bulk lifetime of the *n*-type Cz material, the *p*-*n* junction can be placed either on the front or rear side of the solar cell. Our approach is a back junction solar cell structure using a diffused boron emitter passivated by a dielectric layer [2, 3].
In this article we present our latest results for double side contacted back junction solar cells and give efficiencies for solar cells with rear side aluminum PVD metallization and also for the same solar cell structure with an all screen printed metallization scheme.
In addition to these one sun efficiencies we also show experimental data for low light performances and temperature coefficients and investigate one sun and low light solar cell operation conditions with PC1D modelling.

2 EXPERIMENTAL

Our double side contacted *n*-type Si back junction silicon solar cells are processed in the Reiner-Lemoine Research Center at Hanwha Q CELLS (Thalheim, Germany). We process on *n*-type Cz silicon as base material. If not otherwise stated in the results section a base resistivity of 10 Ω·cm is used. The diffused front and rear side are processed by $POCl_3$ and BBr_3 tube furnace diffusions. The front and the rear side of the solar cells are passivated by dielectric layers. The front side metallization is realized by screen printing. For the rear side metallization we use two different schemes, aluminum deposited by physical vapor deposition (PVD) and all screen printed metallization. A cross section of our back junction solar cell is shown in Figure 1.

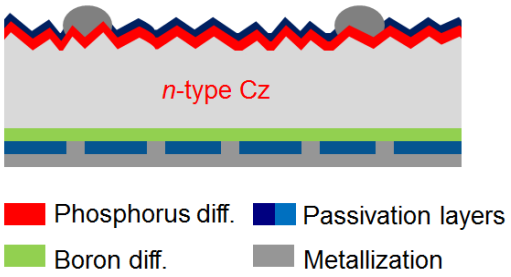

Figure 1: Cross section of the double side contacted back junction solar cell with aluminum rear side metallization

For device simulations we used the numerical device simulation tool PC1D [4]. Simulations were performed for the base resistivities of the experimental data. For the diffused front and rear, parameterizations of experimental diffusion profiles are used. The front reflection is considered using experimental data, too. Surface recombination velocities, diode non-idealities and resistance effects are adjusted to give similar results as experimental solar cells. Concerning the bulk lifetime we assume a constant value of 3 ms after processing.

3 RESULTS

3.1 Analysis of V_{oc} limitations

In order to optimize the efficiency of our solar cell structure, we determined the contributions of front side, rear side and bulk to the total saturation current density J_0 of the solar cell by summation of J_0 data from the different party within the solar cell in a similar way as described in Ref. [5]. The result of this analysis is shown in Figure 1. It is clearly seen, that the metallized surfaces play the main role (55%) in J_0 contributions and therefore are the main limiting factors for the open circuit voltage in our solar cell structure. The passivated surfaces contribute roughly (34%) to the total saturation current density of our solar cell structure. As characteristics of *n*-type silicon material, the bulk only plays a minor role for the total saturation current density of the solar cell.

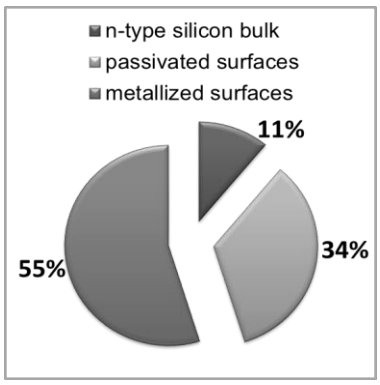

Figure 2: Diagram of the contributions of metallized surfaces, passivated surfaces and silicon bulk to the total saturation current density J_0 at V_{oc} conditions.

3.2 Optimization of cell design

As an example for optimization of our solar cell efficiency, we show the impact of decreasing the front metallization determined from experimental data. A detailed analysis of this experiment is shown in Table I. Here the reduction in metallization fraction by 0.5% absolute is investigated. This reduction resulted in a threefold improvement for our solar cell: the reduced metal fraction causes less optical shading, which leads to an increase in short circuit current density J_{sc}, but in addition to that we also determined an additional increase in J_{sc} and V_{oc} due to reduced recombination. This is clearly a benefit of the solar cell structure based on silicon material with high bulk lifetime as shown in Figure 1: the saturation current density of the bulk plays only a minor role instead of being the main loss contribution as for standard *p*-type BSF solar cells. The reduction in front metallization fraction results in a significant reduction of recombination at the front side of the solar cell and therewith in an increase in open circuit voltage V_{oc}. The additional increase in short circuit current density is specific for our solar cell structure with the emitter on the back side.

3.3 Solar cells with aluminum PVD rear metallization

We applied the optimized metallization scheme shown in the section above to our solar cell structure in combination with a high quality front surface field (FSF), emitter, and passivation layers on front and rear side and achieved a maximum conversion efficiency of 21.3% on a total area of 243.36 cm^2 (Table II). This result was independently confirmed by Fraunhofer ISE CalLab.

Table I: Summary of contributions to efficiency gain due to reduction of screen printed front metallization fraction (determined experimentally).

Reduction of metal fraction	Optical gain in J_{sc}	J_{sc} gain due to reduced recomb.	V_{oc}-gain due to reduced recomb.
[%]	[mA/cm^2]	[mA/cm^2]	[mV]
-0.5	+0.2	+0.2	+2

Table II: *I-V* parameters of our best boron emitter back junction solar cell with rear side aluminum PVD metallization (independently confirmed by Fraunhofer ISE CalLab.)

V_{oc} [mV]	J_{sc} [mA/cm^2]	*FF* [%]	η [%]
673	39.8	79.5	21.3

Table III: *I-V* parameters of our best boron emitter back junction solar cell with all screen printed metallization (independently confirmed by Fraunhofer ISE CalLab)

V_{oc} [mV]	J_{sc} [mA/cm^2]	*FF* [%]	η [%]
671	39.5	78.2	20.7

3.4 Solar cells with all screen printed metallization

In addition to the *n*-type back junction solar cells with PVD rear metallization we also processed solar cells in the same way but with a cost efficient all screen printed metallization. With these solar cells we achieved a maximum conversion efficiency of 20.7% on a total area of 243.36 cm^2. This result also has been independently confirmed by Fraunhofer ISE CalLab (Table III). Both solar cell structures the one with PVD rear metallization and the all screen printed solar cell structure exhibit open circuit voltages larger than 670 mV.

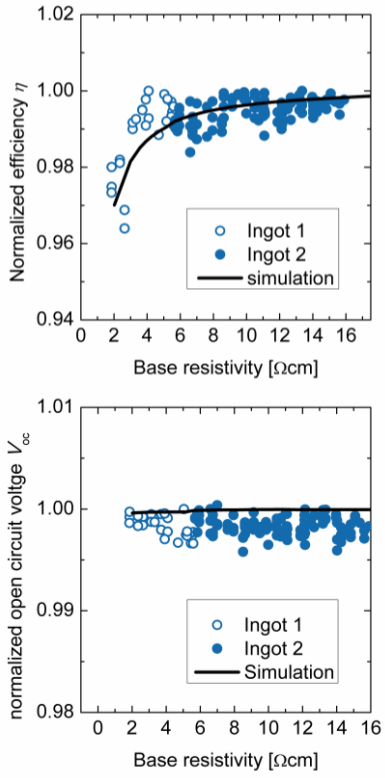

Figure 3: Experimental data and simulations: dependence of normalized efficiency η and open circuit voltage V_{oc} on the base resistivity for the double side contacted back junction solar cell structure. All measurements were performed at 1 sun illumination intensity. For the simulation a constant bulk lifetime of 3 ms is assumed. The data are cited here from reference [6].

3.5 Operation of the solar cell @ 1 sun and 0.1 suns

Recently we published results about the influence of the bulk resistivity impact on the electrical solar cell parameters [6]. One dimensional device simulations using PC1D were compared to experimentally obtained *I-V* parameters (Figure 3). The simulations suggest that our solar cell concept works under high level injection conditions at open circuit voltage which explains the independence of open circuit voltage from bulk resistivity in the range of 2 to 16 Ω·cm. This is demonstrated in the upper graph of Figure 4 showing the simulated excess electron densities (under V_{oc} conditions) compared to the respective bulk doping level for 10 Ω·cm base material.

We also investigated the low light operation of our solar cell structure at an illumination intensity of 0.01 W/m^2 and simulated the excess electron densities at V_{oc} conditions. The respective result is shown in the lower graph of Figure 4. The excess electron density in the bulk is approximately a factor of 2 higher than the base doping concentration which means that the solar cells still operates at close to high injection conditions even at 0.1 suns. The back junction solar cell working conditions at 0.1 suns are therefore similar as determined for 1 sun standard test conditions: depending on base resistivity high level injection respectively close to high level injection conditions are still met under V_{oc} conditions. Therefore, no influence on solar cell operation at lower light intensities is expected. In the next paragraph we give experimental data showing the low light behavior of our solar cells.

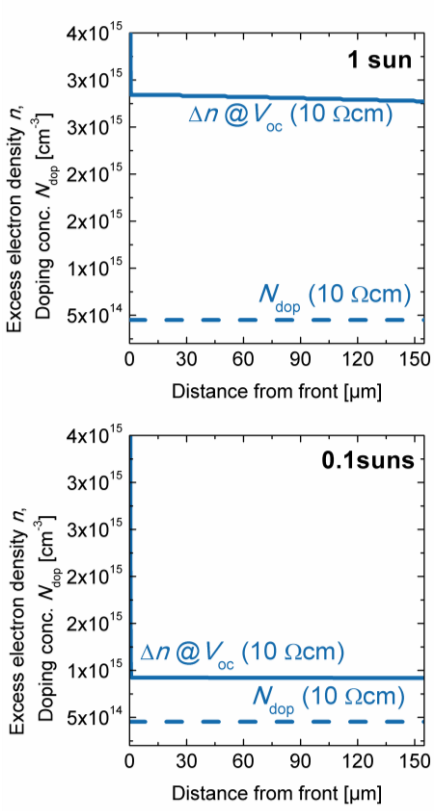

Figure 4: PC1D simulation of excess carrier densities within the bulk for 10 Ω·cm base material at V_{oc} conditions assuming a bulk lifetime of 3 ms: Comparison of excess electron densities Δ*n* and doping concentrations N_{dop} for 1 sun and 0.1 suns illumination intensity.

3.6 Low light performance data and temperature coefficients

We compare standard *p*-type Mono BSF solar cells and our *n*-type double side contacted back junction solar cells on an experimental level. As shown in the graphs in Figure 5, the *n*-type back junction solar cell exhibits a superior low light performance which is mainly related to the better low light behavior of the fill factor. This is caused by the larger series resistance contribution in the solar cell structure coming from the local rear contacts in the solar cell structure. In order to determine the influence of temperature on the operation of our solar cell, we determined the temperature coefficients for our *n*-type back junction solar cell.

The temperature coefficients are given in Table IV in comparison to *p*-type Mono BSF cells. The efficiency loss due to higher temperatures is substantially decreased due to the higher open circuit voltage which was approximately 670 mV whereas the standard *p*-type BSF solar cells show a higher loss with increasing cell temperature.

We note that in addition to the higher efficiency level of the back junction solar cell compared to a standard Mono BSF solar cell the better low light behavior and the more favorable temperature coefficients will also contribute to higher energy yield under identical light conditions.

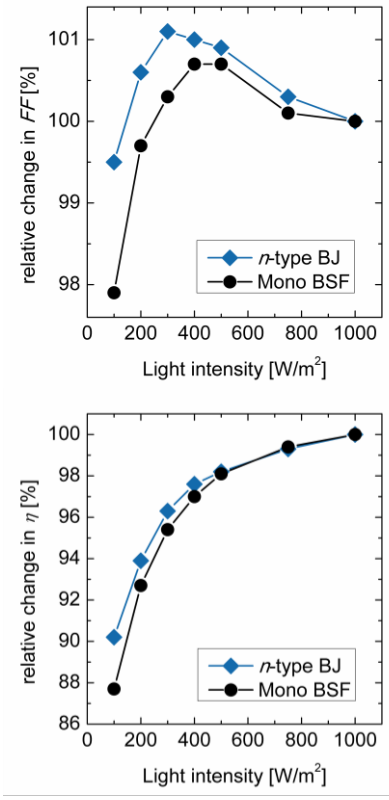

Figure 5: Experimental comparison of solar cell performance for different illumination intensities for *p*-type Mono BSF and *n*-type boron emitter back junction solar cells.

Table IV: Temperature coefficients determined for the individual *I-V* parameters of our *n*-type double side contacted back junction solar cell and for a *p*-type Mono BSF solar cell.

Cell type	T-coeff I_{sc} [%/K]	T-coeff V_{oc} [%/K]	T-coeff P_{mpp} [%/K]
n-type BJ	0.06	-0.31	-0.38
p-type Mono BSF	0.04	-0.33	-0.42

4 SUMMARY

For our boron emitter back junction silicon solar cells featuring both sided contacts and phosphorus diffused front surface field we demonstrated high efficiencies up to 21.3% for rear side aluminum PVD metallization and 20.7% for the same solar cell structure with an all screen printed metallization scheme. Both solar cell structures exhibit high open circuit voltages of larger than 670 mV. By numerical device simulations it was revealed that the solar cells advantages from operating under high level or close to high level injection conditions at 1 sun but also at lower illumination intensities. In addition to the higher absolute efficiency level compared to *p*-type Al-BSF cells we demonstrated positive results for low light performance and temperature coefficients resulting in a higher energy yield of our back junction solar cell structure compared to conventional solar cells with BSF under outdoor test conditions.

5 ACKNOWLEDGEMENTS

The support by the staff of the Reiner Lemoine Research Center at Hanwha Q Cells is gratefully acknowledged.

6 REFERENCES

[1] J. Schmidt, K. Bothe, R. Bock, C. Schmiga, R. Krain, R. Brendel, Proc. 22nd EUPVSEC, Milan, Italy, 2007.
[2] X.M. Dai, M.A. Green, S.R. Wenham, Proc. 23rd IEEE PVSC, Louisville, Kentucky, 1993.
[3] S. Bordihn, V. Mertens, P. Engelhart, T. Florian, J.Cieslak, F. Stenzel, P. Kappe, T. Ballmann, J.Y. Lee, T. Lindner, M. Junghänel, J.W. Müller, W.M.M. Kessels and P. Wawer, Proc. 26th EUPVSEC, Hamburg, Germany, 2011.
[4] P.A. Basore, D.T. Rover, and A.W. Smith, Proc. 20th IEEE PVSC, Las Vegas, Nevada,1988.
[5] S. Kluska, F. Granek, M. Hermle, S. Glunz, Proc. 23rd EUPVSEC, Valencia, Spain, 2008.
[6] V. Mertens, T. Ballmann, J.Y. Lee, M. Junghänel, F. Stenzel, L. Brandt, A. Schulze, P. Engelhart, J.W. Müller, P. Wawer, K.H. Küsters, Energy Procedia, 27, 53-58, 2012.